J Mater Sci: Mater Electron (2015) 26:1102–1106
DOI 10.1007/s10854-014-2511-0

# Preparation and magnetic properties of $Bi_2Fe_4O_9/CoFe_2O_4$ composite powders

**Ying Lin · Pan Kang · Haibo Yang · Miao Liu**

Received: 3 October 2014 / Accepted: 13 November 2014 / Published online: 27 November 2014


**Abstract** $Bi_2Fe_4O_9/CoFe_2O_4$ (BFO/CFO) composite powders were synthesized via a simple one-step sol–gel method. The phase composition and morphology of the as-synthesized composite powders were characterized by an X-ray diffractometer, a Raman spectrometer and a scanning electron microscopy equipped with energy dispersive X-ray spectroscopy respectively, The magnetic properties of the composite powders were investigated by a vibrating sample magnetometer. All the composite powders show single-phase-like magnetic hysteresis loops. The results reveal that the saturation magnetization ($M_s$), the remnant magnetization ($M_r$), and the coercivity ($H_c$) all increase with increasing the concentration of CFO.

## 1 Introduction

Ternary bismuth ferrites have attracted much attention in recent years because of their promising and potential applications in sensor, actuation, and digital memory [1–4]. As a typical bismuth ferrite, $Bi_2Fe_4O_9$ (BFO) is known to have an orthorhombic structure with lattice constants of a = 7.965 Å, b = 8.440 Å and c = 5.994 Å, whose unit cell contains two formula units with trivalent Fe ions distributed between the octahedral and tetrahedral sites respectively. Thus BFO belongs to Fe-based magnetic Cairo pentagonal lattice leading to a spin frustration [5]. It is paramagnetic at room temperature and undergoes a transition to an antiferromagnetic state at $T_N = 264 \pm 3$ K. Nowadays, BFO has been cited as a promising material not only for its multiferroic behavior [6] but has also been used as high-performance semiconductor gas sensors and other functional devices [7–9]. However, the applications are seriously restricted by the deficiency of weak macroscopic magnetism. Hence, it is necessary to improve the magnetic properties of BFO.

Previous studies on improving the magnetic properties of BFO mainly focused on changing the overall magnetic spin structure and inducing magnetization in BFO, through doping with several transition metal ions [10–12]. However, doping with transition metal ions could not significantly improve the magnetic properties of BFO. Obviously, Compositing might be one of good solutions to achieve the goal. The composites are artificial systems containing at least two phases with different physical and chemical properties separated at microscopic level in the final product, which are attracting an increasing interest in view of various applications [13]. Spinel $CoFe_2O_4$ (CFO) is a well-known magnetic material, which has been studied in detail due to its high saturation magnetization (about 80 emu/g).

The aim of this paper is to composite CFO into BFO to improve the magnetic properties of BFO. The BFO/CFO composite powders were synthesized using a one-step sol–gel method. It is interesting that the pure-phase BFO/CFO composite powder can be obtained by calcining the gel containing the starting materials of BFO and CFO with different mass ratios of BFO and CFO at a low temperature. The magnetic properties of the as-prepared BFO/CFO composite powders increase significantly with increasing the concentration of CFO.

Y. Lin · P. Kang · H. Yang (✉) · M. Liu
School of Materials Science and Engineering, Shaanxi University of Science and Technology, Xi'an 710021, China
e-mail: yhb1-1-1@163.com

Y. Lin
Shaanxi Research Institute of Agricultural Products Processing Technology, Xi'an 710021, China

## 2 Experimental procedure

(1 − x)BFO/xCFO composite powders (with x = 10, 20, 30, 40 %,) were synthesized by a one-step sol–gel method. The starting reagents were analytical grade bismuth nitrate ($Bi(NO_3)_3{\cdot}5H_2O$), ferric nitrate ($Fe(NO_3)_3{\cdot}9H_2O$), cobalt nitrate ($Co(NO_3)_2{\cdot}6H_2O$), citric acid ($C_6H_8O_7{\cdot}H_2O$) and ethylenediamine ($C_2H_8N_2$). Then ferric nitrate, bismuth nitrate and cobalt nitrate were weighed and added into the citric acid solution and magnetically stirred at 25 °C, according to the stoichiometry of (1 − x)BFO/xCFO composite powders (with x = 10, 20, 30, 40 %). The addition of 5 % mol excess bismuth nitrate was used to compensate the Bi loss during the subsequent calcination. Ethylenediamine was added to the above solution to adjust the pH value and thus inhibit the hydrolyzation of Bi. After that the mixture solution was dried at 200 °C for 2 h to obtain the BFO/CFO precursor powders [14]. Finally, the precursor powders were calcined at different temperatures to obtain the BFO/CFO composite powders. The phase composition of the BFO/CFO composite powders were detected by an X-ray diffractometer (XRD) with Cu Kα radiation (Rigaku D/MAX-2400, Japan) and a micro Raman spectrometer with a 514 nm $Ar^+$ laser (Renishaw-invia, England). The morphology of the composite powders was analyzed using a scanning electron microscope (SEM) (JEOL JSM-6390A JEOL Ltd, Tokyo) equipped with an energy dispersive X-ray spectroscopy (EDS). The magnetic hysteresis loops of the composite powders were measured by a vibrating sample magnetometer 113 (VSM) (Lake Shore 7410, USA).

## 3 Results and discussion

Figure 1 shows the XRD patterns of the 80 %BFO/20 %CFO composite powders calcined at different temperatures ranged from 600 to 750 °C for 2 h. As shown in Fig. 1, the phase composition of the as-prepared composite powder is sensitive to the variation of calcining temperature. For the sample calcined at 600 °C, besides the main phases of BFO and CFO, the impurity phases of $BiFeO_3$ and unreacted $Fe_2O_3$ can also be detected. With increasing the calcining temperature to 650 °C, the diffraction peaks of $Fe_2O_3$ disappear. With further increasing the calcining temperature the diffraction peaks of BFO and CFO becomes strengthened gradually.

The XRD patterns of the BFO/CFO composite powders with different concentrations of CFO calcined at 750 °C for 2 h are shown in Fig. 2. It can be clearly seen that only the expected phases of BFO and CFO can be detected in all the samples. Moreover, the XRD patterns show that the synthesized powders of BFO and CFO are of pure

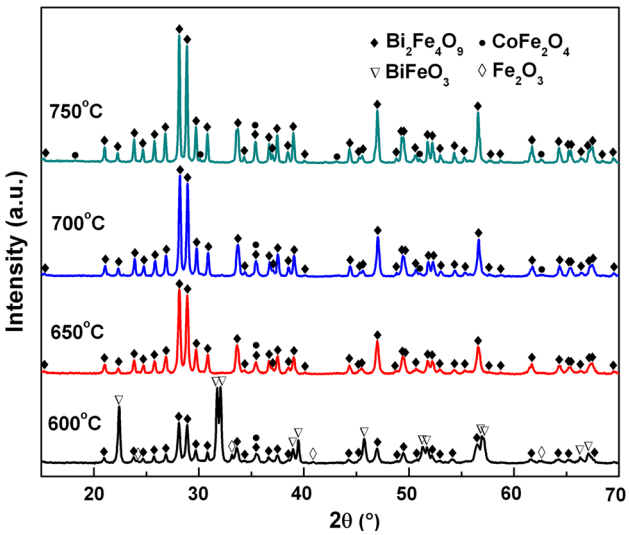


**Fig. 1** XRD patterns of the 80 %BFO/20 %CFO composite powders calcined at different temperatures

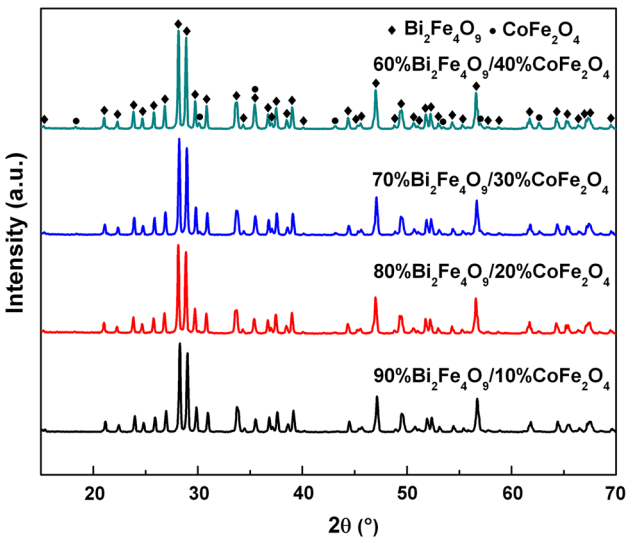


**Fig. 2** XRD patterns of the BFO/CFO composite powders with different concentrations of CFO

rhombohedral distortion perovskite structure and cubic structure, respectively. Within the resolution limit of XRD no any other immediate phase can be detected. The above powder X-ray diffractograms reveal that BFO and CFO phases co-exist after being calcined at 750 °C with a high crystallinity and without any impurity phases. Obviously, with increasing the concentration of CFO, the diffraction peaks of CFO become strengthened gradually.

It is hard to distinguish γ-$Fe_2O_3$ phase from CFO phase using XRD technique [15]. Thus further confirming the phase purity of the sample and excluding the interference of γ-$Fe_2O_3$ phase on the magnetic properties of the BFO/CFO composite powders is necessary. Raman spectra of

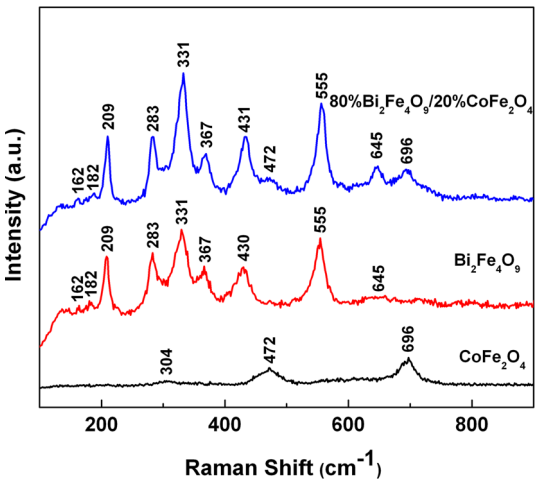


**Fig. 3** Raman spectra of the BFO powder, CFO powder and 80 %BFO/20 %CFO composite powder

the pure phase BFO, CFO and the 80 %BFO/20 %CFO composite powders were measured at room temperature as presented in Fig. 3. A group theory treatment leads to 42 Raman active modes for BFO ($12A_g + 12B_{1g} + 9B_{2g} + 9B_{3g}$) and five Raman active modes for CFO ($A_{1g} + E_g + 3T_{2g}$) [16, 17]. Three modes at 304, 472, 696 $cm^{-1}$ can be found in the pure CFO powder. And there are eleven modes at 162, 182, 209, 283, 331, 367, 430, 555, 645 $cm^{-1}$ in the pure phase BFO powder. Almost all the modes which appear in BFO and CFO powders can be seen except a mode of CFO at 304 $cm^{-1}$ in the composite powders, which might be obscured by other modes. The above observation indicates that the composite powders do not contain $\gamma$-$Fe_2O_3$ phase. Hence, based on the above XRD and Raman analysis, it can be concluded that the as-prepared BFO/CFO composite powders are very pure.

Figure 4 shows the SEM micrographs of the BFO/CFO composite powders with different concentrations of CFO calcined at 750 °C for 2 h. It can be found that the small grains are of CFO phase while the large grains are of BFO phase because the formation temperature of CFO is higher than that of BFO [18, 19]. The grain sizes of BFO and CFO are about 300–400 and 100 nm, respectively. Figure 5 shows EDS mapping analysis result of the representative 80 %BFO/20 %CFO composite powder. It can be found that the atomic ratio of Bi/Fe approximately is 0.435, which is close to the stoichiometric ratio value of 0.444. As shown in the mapping analysis, it can be clearly seen that all the related elements are distributed uniformly, confirming that the two phases are well distributed in the composite powders.

Figure 6 shows the magnetic hysteresis loops of the BFO/CFO composite powders with different concentrations of CFO. It shows obviously enhanced ferromagnetic properties and the magnetic properties of the BFO/CFO composite powders are strongly dependent on the concentration of CFO. It indicates that the saturation magnetization ($M_s$), the remnant magnetization ($M_r$), and the

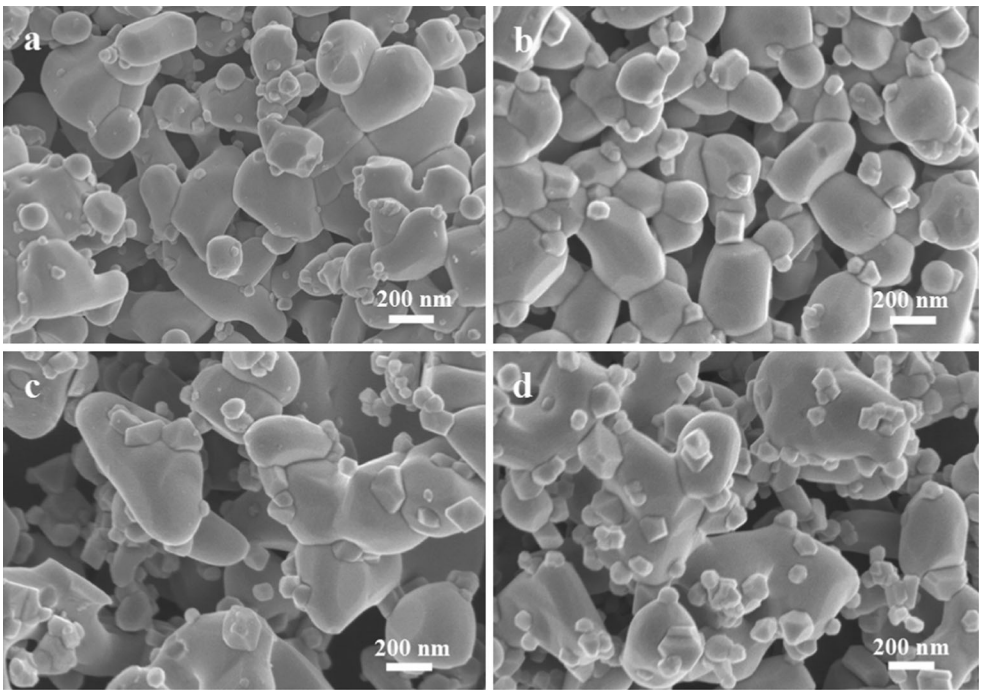


**Fig. 4** SEM micrographs of the BFO/CFO composite powders with different concentrations of CFO: **a** 90 %BFO/10 %CFO; **b** 80 %BFO/20 %CFO; **c** 70 %BFO/30 %CFO; **d** 60 %BFO/40 %CFO

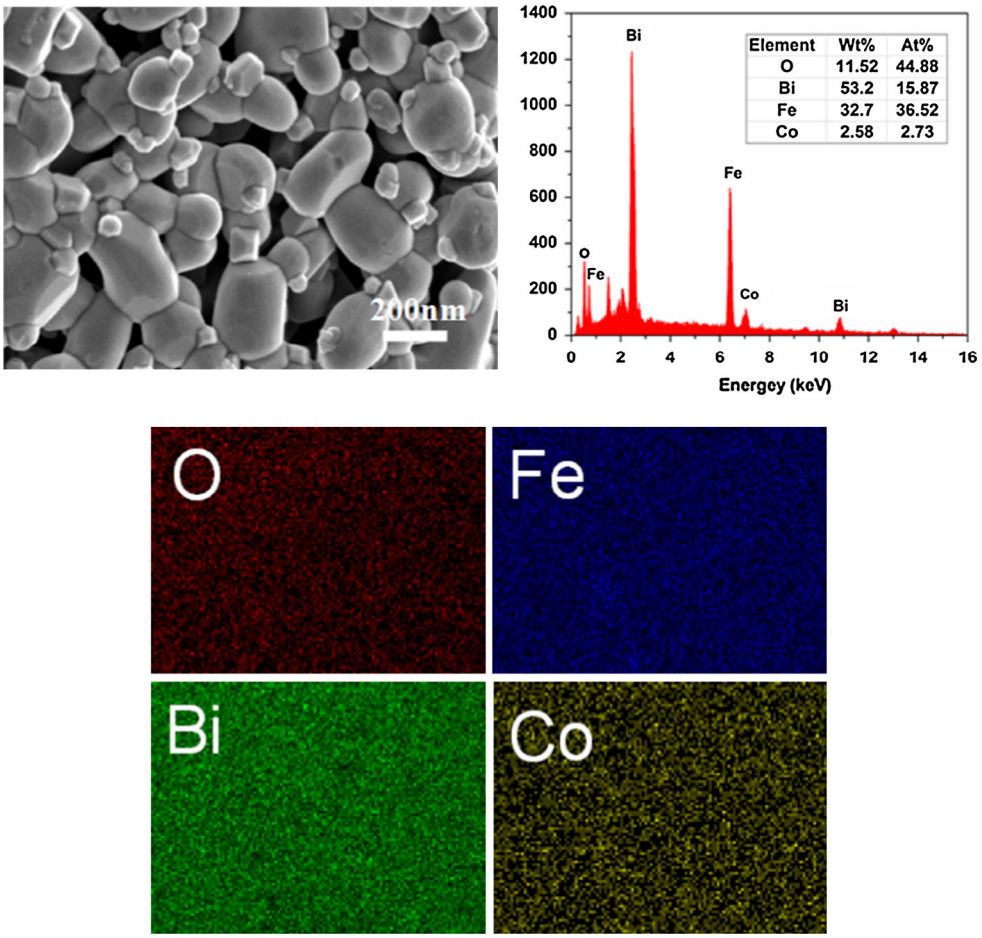


**Fig. 5** EDS mapping analysis result of the 80 %BFO/20 %CFO composite powder

coercivity ($H_c$) all increase with increasing the concentration of CFO. This phenomenon is due to the fact that the CFO is a classical magnetic ferrite while the BFO is of antiferromagnetic nature [20–22]. Table 1 summarizes the magnetic properties of the as-prepared BFO/CFO composite powders and those of the doped BFO powders

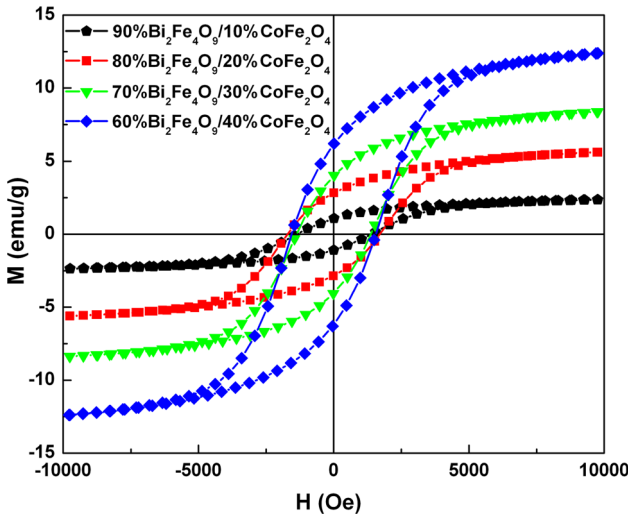


**Fig. 6** Magnetic hysteresis loops of the BFO/CFO composite powders with different concentrations of CFO

**Table 1** Magnetic properties of the BFO/CFO composite powders and the doped BFO powders

| Samples | $M_s$ (emu/g) | $M_r$ (emu/g) | $H_c$ (Oe) | Ref. |
|---|---|---|---|---|
| $Bi_2Fe_4O_9$ (297 K) | ~0.032 | ~0.005 | ~200 | [14] |
| $Bi_2Fe_{3.9}Sc_{0.1}O_9$ (297 K) | ~0.166 | ~0.008 | – | [11] |
| $Bi_2Fe_{3.8}Ti_{0.1}O_9$ (297 K) | ~0.248 | ~0.029 | – | [23] |
| $Bi_2Fe_{3.95}Co_{0.05}O_9$ (5 K) | ~3.509 | ~1.466 | ~1,010.2 | [12] |
| 90 %BFO/10 %CFO (297 K) | ~2.036 | ~1.091 | ~1,388.4 | This work |
| 80 %BFO/20 %CFO (297 K) | ~4.816 | ~2.875 | ~1,660.8 | This work |
| 70 %BFO/30 %CFO (297 K) | ~7.294 | ~4.042 | ~1,448.1 | This work |
| 60 %BFO/40 %CFO (297 K) | ~10.856 | ~6.129 | ~1,575.8 | This work |

reported in literatures. It can be clearly seen that all the magnetic properties ($M_s$, $M_r$ and $H_c$) are much higher than those of the doped BFO powders, suggesting that compositing CFO into BFO is a good solution to enhance the magnetic properties of BFO.

## 4 Conclusions

In this work, the BFO/CFO composite powders have been successfully synthesized by a one-step sol–gel method. XRD and Raman results reveal that the BFO and CFO phase can co-exist in the composite powders without any impurity phase. Moreover, the results of SEM and EDS show that the two phases are well distributed in the composite powders. Magnetic hysteresis loops of the BFO/CFO composite powders indicate that the $M_s$ and $H_c$ of the BFO/CFO increase significantly with increasing the concentration of CFO. Compositing CFO into BFO is a good solution to enhance the magnetic properties of BFO.

**Acknowledgments** This work is supported by the National Natural Science Foundation of China (Grant No. 51402178), the Science and Technology Foundation of Shaanxi Province (Grant No. 2013KJXX79, 2013JQ6004) and the Special Foundation of the Ministry of Shaanxi Province (Grant No. 2013JK0937) and the Scientific Research Starting Foundation of Shaanxi University of Science and Technology (Grant No. BJ13-13).

## References

1. W. Eerenstein, N.D. Mathur, J.F. Scott, Nature **442**, 759–765 (2006)
2. M. Yasin Shami, M.S. Awan, M. Anis-ur-Rehman, J. Electron. Mater. **41**, 2216–2224 (2012)
3. M. Valant, D. Suvorov, Chem. Mater. **14**, 3471 (2002)
4. D. Voll, A. Beran, H. Schneider, Phys. Chem. Miner. **33**, 623 (2006)
5. H. Koizumi, N. Niizeki, T. Ikeda, Jpn. J. Appl. Phys. **3**, 495 (1964)
6. A.K. Singh, S.D. Kaushik, B. Kumar, P.K. Mishra, A. Venimadhav, V. Siruguri, Appl. Phys. Lett. **92**, 132910 (2008)
7. Z. Yang, Y. Huang, B. Dong, H.L. Li, S.Q. Shi, J. Solid State Chem. **179**, 3324–3329 (2006)
8. A.S. Poghossian, H.V. Abovian, P.B. Avakian, S.H. Mkrtchian, V.M. Haroutunian, Sens. Actuators B **4**, 545–549 (1991)
9. H.J. Sun, Y. Liu, Y. Zhang, L. Lv, J. Zhou, W. Chen, J. Mater. Sci. Mater. Electron. **25**, 4212–4218 (2014)
10. Y. Du, Z.X. Cheng, S.X. Dou, X.L. Wang, Mater. Lett. **64**, 2251–2253 (2010)
11. D.P. Dutta, C. Sudakar, P.S.V. Mocherla, B.P. Mandal, O.D. Jayakumar, A.K. Tyagi, Mater. Chem. Phys. **135**, 998–1001 (2012)
12. M. Liu, H.B. Yang, Y. Lin, Y.Y. Yang, J. Mater. Sci. Mater. Electron. doi:10.1007/s10854-014-2256-9
13. C.E. Ciomaga, M. Airimioaei, V. Nica, L.M. Hrib, O.F. Caltun, A.R. Lordan et al., J. Euro. Ceram. Soc. **32**, 3325–3327 (2012)
14. M. Zhang, H. Yang, T. Xian, Z.Q. Wei, J.L. Jiang, Y.C. Feng, J. Alloys Compd. **509**, 809–811 (2011)
15. J. Chen, Y. Wang, Y. Deng, J. Alloys Compd. **552**, 65–69 (2013)
16. M.N. Iliev, A.P. Litvinchuk, V.G. Hadjiev, M.M. Gospodinov, V. Skumryev, E. Ressouche, Phys. Rev. B **81**, 024302 (2010)
17. L.V. Gasparov, D.B. Tanner, D.B. Romero, H. Berger, G. Margaritondo, L. Forro, Phys. Rev. B **62**, 7939–7944 (2010)
18. T. Liu, Y.B. Xu, C.L. Zeng, Mater. Sci. Eng., B **176**, 535–539 (2011)
19. X.Y. Wu, H.B. Yu, H. Deng, Ceram. Int. **40**, 12883–12889 (2014)
20. G.C.P. Leite, E.F. Chagas, R. Pereira, R.J. Prado, A.J. Terezo, M. Alzamora, E. Baggio-Saitovitch, J. Magn. Magn. Mater. **324**, 2711–2716 (2012)
21. H. Dong, A. Meininger, H.J. Jiang, K.-S. Moon, C.P. Wong, J. Electron. Mater. **36**, 593–597 (2007)
22. J.G. Lee, H.M. Lee, C.S. Kim, O.Y. Jei, J. Magn. Magn. Mater. **177–181**, 900–902 (1998)
23. Z.M. Tian, Y. Qiu, S.L. Yuan, M.S. Wu, S.X. Huo, H.N. Duan, J. Appl. Phys. **108**, 064110 (2010)